

Quenching of Singlet Molecular Oxygen, $O_2(a^1\Delta_g)$ and $O_2(b^1\Sigma_g^+)$, by H_2 , D_2 , HCl and HBr

Peter Borrell† and Donald S. Richards‡

Department of Chemistry, Keele University, Staffordshire ST5 5BG

Using a discharge flow/shock tube measurements have been made of the quenching of $O_2(a^1\Delta_g)$ and $O_2(b^1\Sigma_g^+)$ by H_2 and D_2 at 292 K and between 500 and 1000 K. Results are also reported for the quenching of $O_2(b^1\Sigma_g^+)$ by HCl over a similar temperature range and by HBr at 292 K. No measurements were possible for HBr at high temperatures. The two excited states differ in the temperature dependence of their quenching rate constants: the results for $O_2(a^1\Delta_g)$ can be fitted approximately to the Arrhenius equation, while those for $O_2(b^1\Sigma_g^+)$ change only slightly with temperature. The results are considered in terms of current models for electronic energy transfer.

The two low-lying excited states of singlet molecular oxygen continue to offer a challenge to the understanding of their collisional deactivation. Both are extraordinarily stable,¹ having long radiative lifetimes. $O_2(a^1\Delta_g)$ is less susceptible to collisional deactivation than $O_2(b^1\Sigma_g^+)$, but the quenching ability of particular gases for the two is quite unpredictable: CO_2 , for example, is an efficient quencher of $O_2(b^1\Sigma_g^+)$ but is so poor a quencher of $O_2(a^1\Delta_g)$ that the rate constant is difficult to measure.¹ Our own work has been devoted to measuring the temperature dependence of the quenching reactions at both high^{2,3} and low temperatures⁴ and, here again, the two states differ markedly: the $O_2(a^1\Delta_g)$ state displays an approximately Arrhenius behaviour for several quenchers, while the rate constants for the quenching of $O_2(b^1\Sigma_g^+)$ are nearly independent of temperature.

Maier and co-workers^{5,6} have shown a possible path to understanding this behaviour in their recent experimental and theoretical studies of the quenching of both states by oxygen itself at low temperatures. The rate constants for the quenching by the two isotopic forms, $^{16}O_2$ and $^{18}O_2$, could be interpreted in terms of a model in which the electronic energy is distributed between the vibrations of the two colliding molecules.

In the present work we have studied the quenching of both states by H_2 and D_2 since the results with these quenchers should offer a tractable challenge to the theorist. Some single-temperature measurements of the rate constants have been made previously (see the Discussion for details) as has a measurement of the temperature dependence of the quenching of the $O_2(b^1\Sigma_g^+)$ state over a limited temperature range. However, several of the earlier results have had to be revised, so it was clearly worthwhile to re-measure the rates at room temperature and to study the temperature dependence over as wide a range as possible. The results illustrate further the differing behaviour of the two states.

We also report on the results of high-temperature experiments with HCl , and a room-temperature value for the quenching of $O_2(b^1\Sigma_g^+)$ by HBr .

† Present address: Fraunhofer Institute for Atmospheric Environmental Research, Hindenburgstrasse 43, D8100 Garmisch-Partenkirchen, Federal Republic of Germany.

‡ Present address: Leda-Mass, Knypersley, Stoke-on-Trent ST8 7TY.

Experimental

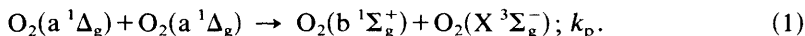
The measurements were made by observing the changes of emission intensity from excited oxygen on the addition of the quencher, using the combined discharge flow/shock tube apparatus which has been described in detail previously.^{7,8}

Singlet oxygen is generated by passing a flow of purified oxygen (*ca.* 9 mmol s⁻¹), at typically 800 Pa (6 Torr) pressure, over a mercury pool and through the cavity of a microwave discharge (2450 MHz; 100 W). The flow, which then contains *ca.* 5% of O₂(a ¹Δ_g), is passed into the test section of a 5 m long glass shock tube which is 5 cm in diameter.

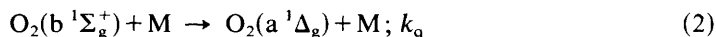
The oxygen was passed through a 1 m column of molecular sieve and a liquid-nitrogen-cooled trap for purification. H₂ and D₂ were treated similarly. HCl and HBr were purified by distillation.

The quenching of O₂(a ¹Δ_g) at room temperature⁹ is studied by measuring the fall in concentration over a 1 m length of the tube, situated *ca.* 0.5 m beyond the inlet to the tube and *ca.* 1 m from the discharge. The concentration is monitored with the 'dimol' emission, using a 634 nm filter with a 10 nm half-height width, and a photomultiplier (EMI 9658B).

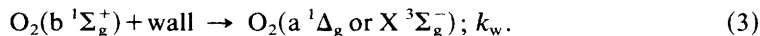
O₂(b ¹Σ_g⁺) is generated⁹ in the flow itself by an energy-pooling reaction



It is removed by quenching with either oxygen or the test gas,



or by collision with the tube wall



A steady state is maintained at each point in the flow so that the concentration of O₂(b ¹Σ_g⁺) is given by

$$[\text{O}_2(\text{b } ^1\Sigma_{\text{g}}^+)] = k_{\text{p}}[\text{O}_2(\text{a } ^1\Delta_{\text{g}})]^2 / (k_{\text{q}}[\text{M}] + k_{\text{w}}) \quad (4)$$

The concentration is monitored with the emission from the single molecule (b → X) transition at 762 nm, and the quenching studied by observing the relative changes in the emissions at 762 and 634 nm at a single point in the tube as the concentration of quencher is varied.

After first establishing the flow conditions and measuring the concentration gradient in the pre-shock flow with the travelling photomultiplier, the high-temperature measurements were made by passing a shock wave into the gas in the opposite direction to the pre-shock flow.^{7,8} The shock wave is initiated by bursting naturally an aluminium diaphragm with *ca.* 6 atm[†] of helium or nitrogen. The velocity, from which the post-shock conditions are calculated,⁷ is measured with laser light screens. Photomultipliers with 634 or 762 nm filters are used to observe the emission; the output signals are digitised and stored with transient recorders, and emission records are subsequently passed to the main computer for treatment by a combination of computer graphics and non-linear least-squares techniques.¹⁰

Results

Rate Constants for the Quenching of O₂(a ¹Δ_g) by H₂ and D₂ at 292 K

In the pre-shock flow, O₂(a ¹Δ_g) is deactivated by collision with O₂, with the quencher, Q, or at the tube wall. All of these processes are first-order with respect to [O₂(a ¹Δ_g)],

[†] 1 atm = 101 325/760 Pa.

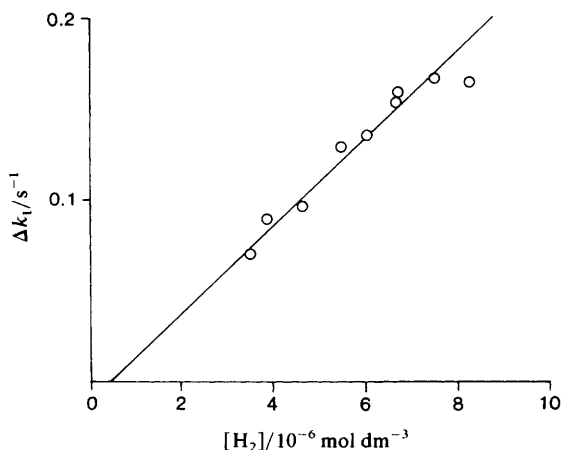


Fig. 1. Second-order plot for the quenching of $\text{O}_2(\text{a } ^1\Delta_g)$ by H_2 .

so that the first-order decay constant, k_1 , is given in terms of the quenching rate constants and the emission intensity, I_b , at a distance, l , down the tube by:

$$k_1 = (k_d[\text{O}_2] + k_d^Q[\text{Q}] + k_w^\Delta) = (v/l) \ln(I_l/I_{l=0})$$

where v is the linear flow velocity. Good first-order plots were obtained for both pure oxygen and oxygen with the added quenchers, and the value of k_d^Q for each quencher was obtained by plotting Δk_1 , the difference in k_1 with and without quencher, against $[\text{Q}]$.

Such a plot for H_2 is shown in fig. 1 and the slope gives the quenching rate constant to be

$$\text{O}_2(\text{a } ^1\Delta_g) + \text{H}_2: \quad k_d^{\text{H}_2} = (2.20 \pm 0.30) \times 10^4 \text{ dm}^3 \text{ mol}^{-1} \text{ s}^{-1}$$

where the error limits are 2σ values.

Our experiments were directed towards high-temperature studies so we deliberately restricted the concentration range of H_2 and D_2 to $<5\%$ of the O_2 to reduce the possibility of explosions. Since H_2 is a relatively efficient quencher, this limitation posed no problems, but difficulties were encountered with D_2 , which proved to be a poor quencher. With D_2 there were only small differences in slope between the first-order plots with and without quencher, and so the values of Δk_1 on the second-order plot were scattered. Finally, after 28 runs, $k_d^{\text{D}_2}$ was determined for each run and the values were then averaged to give:

$$\text{O}_2(\text{a } ^1\Delta_g) + \text{D}_2: \quad k_d^{\text{D}_2} = (2.6 \pm 1.3) \times 10^3 \text{ dm}^3 \text{ mol}^{-1} \text{ s}^{-1}.$$

The large error limits reflect the scatter of the results.

Quenching Rate Constants for $\text{O}_2(\text{b } ^1\Sigma_g^+)$ at 292 K

The ratio of the emissions at 634 nm and 762 nm, ϕ , is given by:

$$\phi = a[\text{O}_2(\text{a } ^1\Delta_g)]^2/[\text{O}_2(\text{b } ^1\Sigma_g^+)] \quad (6)$$

where a is a constant depending on geometry of the detection arrangement *etc.* If eqn (6) is combined with eqn (4), ϕ_Q , the emission ratio in the presence of the quencher Q, becomes:

$$\phi_Q = a(k_q^{\text{O}_2}[\text{O}_2] + k_q^Q[\text{Q}] + k_w)/k_p. \quad (7)$$

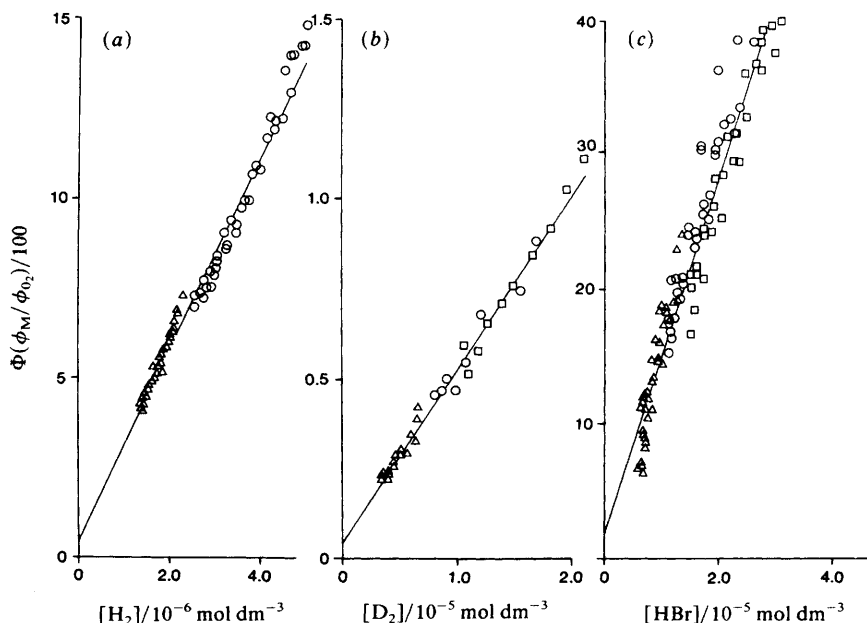


Fig. 2. Plots of $\Phi(\phi_Q, \phi_0)$ against concentration for runs with (a) H_2 , (b) D_2 and (c) HBr . The slopes give the rate constants for quenching of $\text{O}_2(\text{b } ^1\Sigma_g^+)$; Mixtures used; H_2 : Δ , 0.5%; \circ , 1%; D_2 : Δ , 1.5%; \circ , 3.5%; \square , 4.5%; HBr : Δ , 3%; \circ , 5%; \square , 7%.

The quenching rate constant, k_q , can then be expressed in terms of the emission ratios in the presence and absence of the quencher, ϕ_Q and ϕ_0 :

$$k_q^Q[\text{Q}] = \{(k_q^{\text{O}_2}[\text{O}_2] + k_w^0)(\phi_Q - \phi_0)/\phi_0\} - (k_w - k_w^0) \\ = \Phi(\phi_Q, \phi_0) \quad (8)$$

where k_w and k_w^0 are the wall constants in the presence and absence of quencher. These were estimated from the equation for diffusion in a circular tube given by Derwent and Thrush;¹¹ the value of $k_q^{\text{O}_2}$, the quenching value for O_2 alone,⁷ was taken to be $1.00 \times 10^5 \text{ dm}^3 \text{ mol}^{-1} \text{ s}^{-1}$.

Fig. 2 shows plots of $\Phi(\phi_Q, \phi_0)$ against $[\text{Q}]$ for H_2 , D_2 and HBr determined from results with several mixtures. Good results were obtained and the slopes of the plots give the rate constants to be:

$$\text{O}_2(\text{b } ^1\Sigma_g^+) + \text{H}_2: \quad k_q^{\text{H}_2} = (2.8 \pm 0.1) \times 10^8 \text{ dm}^3 \text{ mol}^{-1} \text{ s}^{-1}$$

$$\text{O}_2(\text{b } ^1\Sigma_g^+) + \text{D}_2: \quad k_q^{\text{D}_2} = (5.3 \pm 0.2) \times 10^6 \text{ dm}^3 \text{ mol}^{-1} \text{ s}^{-1}$$

$$\text{O}_2(\text{b } ^1\Sigma_g^+) + \text{HBr}: \quad k_q^{\text{HBr}} = (1.42 \pm 0.1) \times 10^8 \text{ dm}^3 \text{ mol}^{-1} \text{ s}^{-1}.$$

A value for HCl has been reported previously.^{9,12} Since measurements for the quenching of $\text{O}_2(\text{b } ^1\Sigma_g^+)$ are taken at a single point in the tube, and the relative concentrations of $\text{O}_2(\text{a } ^1\Delta_g)$ and $\text{O}_2(\text{b } ^1\Sigma_g^+)$ measured simultaneously, the results for HCl and HBr are not subject to changing wall reactions in the presence of these gases which Singh *et al.*¹³ found affected measurements of the quenching of $\text{O}_2(\text{a } ^1\Delta_g)$.

High-temperature Quenching of $\text{O}_2(\text{a } ^1\Delta_g)$ by H_2 and D_2

The high-temperature rate constants for the quenching of $\text{O}_2(\text{a } ^1\Delta_g)$ were estimated by monitoring the emission at 634 nm in the post-shock regime. The emission rose sharply

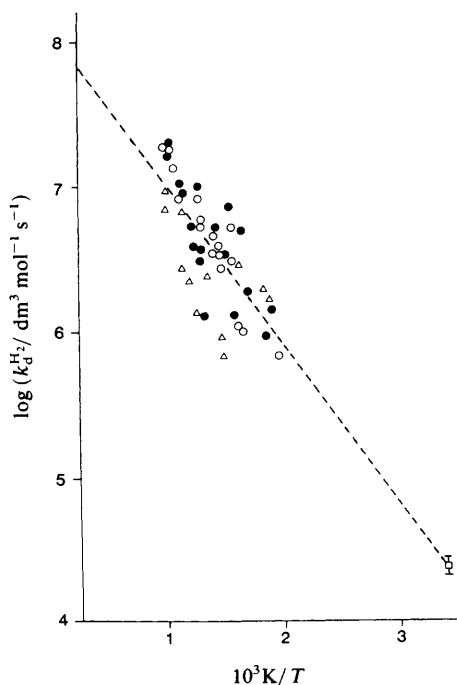


Fig. 3. An Arrhenius plot for the quenching of $O_2(a^1\Delta_g)$ by H_2 . Mixtures used in oxygen: \circ , 0.5%; \bullet , 1%; \triangle , 1% in a 3:1 O_2/N_2 mixture. \square , room temperature measurement.

at the shock front and then decayed exponentially. As has been found previously, the emission could be described⁸ by:

$${}^{634}I(t) = {}^{634}I_{\text{psg}} \left(\frac{\rho_2}{\rho_1} \right)^2 \left(\frac{T_2}{T_1} \right)^{1/2} \frac{K}{t_s} \int_{t-t_s}^t \exp(-\beta t) dt \quad (9)$$

${}^{634}I(t)$ and ${}^{634}I_{\text{psg}}$ are the post- and pre-shock emission intensities; ρ_2/ρ_1 and T_2/T_1 are the ratios of the post- to pre-shock densities and temperatures; K is the enhancement factor which here expresses the ratio of the dimol emission rate constant at high temperature to that at low temperature; t_s is the integration time for the optical system, and β is the observed post-shock decay constant.

There are two contributions to the decay constant, β : the pre-shock concentration gradient of $O_2(a^1\Delta_g)$ in the shock tube, and the deactivation of $O_2(a^1\Delta_g)$ at the shock temperature:

$$\beta = u\alpha[(\rho_2/\rho_1)-1] + k_d^Q[Q] \quad (10)$$

where u is the shock velocity and α is the constant describing the pre-shock decay along the tube.⁸

The experimental traces are fitted to eqn (9) using a non-linear least-squares analysis which yields K , t_s and β . The values found for K and t_s provide a check on the quality of the experiment; the rate constant is then determined from β using eqn (10). The quenching by oxygen itself and by the wall can be neglected at high temperatures.⁷

Fig. 3 and 4 show the results for the quenching of $O_2(a^1\Delta_g)$ by H_2 and D_2 as Arrhenius plots over the temperature range 292–1000 K. While the majority of the experiments were made by adding H_2 or D_2 to purified oxygen, some were made by adding the quencher to a 1:3 N_2 – O_2 mixture in an attempt to reduce the additional emission,

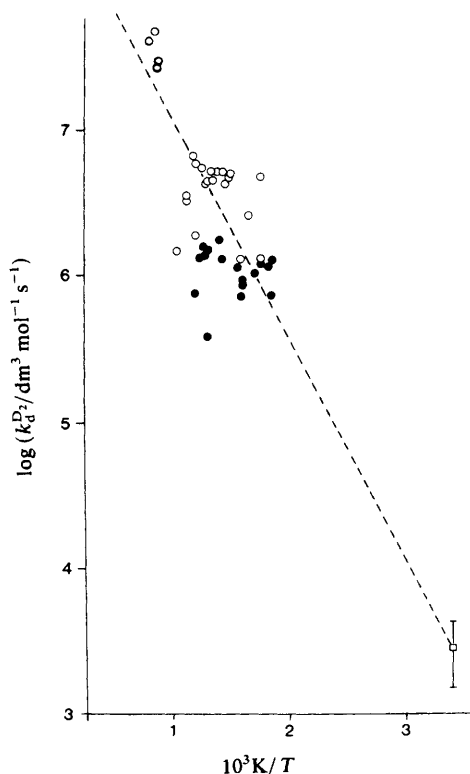


Fig. 4. An Arrhenius plot for the quenching of $\text{O}_2(\text{a } ^1\Delta_g)$ by D_2 . Mixtures used in an $\text{O}_2\text{-N}_2$ mixture: \circ , 1.5%; \bullet , 3%. \square , Room temperature measurement.

mentioned below, and so extend the temperature range. Unfortunately there is an appreciable scatter because the differences between the observed decay constants and the contributions from the pre-shock gradient, (10), are small and so the experimental uncertainties are magnified. The scatter prevents the detailed form of the temperature dependence from being discerned but the data can be fitted to the Arrhenius equation. The equations for the rate constants are:

$$\text{O}_2(\text{a } ^1\Delta_g) + \text{H}_2: \quad k_q^{\text{H}_2} = (1.3 \pm 1.0) \times 10^8 \exp [-(2600 \pm 200)/T] \text{ dm}^3 \text{ mol}^{-1} \text{ s}^{-1}$$

$$\text{O}_2(\text{a } ^1\Delta_g) + \text{D}_2: \quad k_q^{\text{D}_2} = (2.9 \pm 1.2) \times 10^8 \exp [-(3400 \pm 200)/T] \text{ dm}^3 \text{ mol}^{-1} \text{ s}^{-1}.$$

Additional Emission

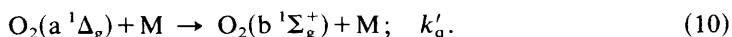
The upper temperatures for which H_2 and D_2 could be studied were limited by additional emission which appeared on the traces as a peak *ca.* 350 μs behind the shock front for runs at 1000 K. As the temperature was raised, the delay shortened and the peak height increased. The new feature is presumably due to combustion of H_2 or D_2 at the shock temperature.

High-temperature Quenching of $\text{O}_2(\text{b } ^1\Sigma_g^+)$

The emission traces at 762 nm from $\text{O}_2(\text{b } ^1\Sigma_g^+)$ have a different appearance^{7,8} from those at 634 nm. After the initial rise due to shock compression, the emission increases further

before passing through a maximum and then decaying. The enhancement of the emission is due to the shift in the steady-state concentration of $O_2(b^1\Sigma_g^+)$, eqn (4), as the pooling constant, k_p , increases more rapidly with temperature than the quenching constant, k_q . The fall off, as with the 634 nm emission, is due to the pre-shock concentration gradient of $O_2(a^1\Delta_g)$ in the tube.

A recent re-analysis of our earlier work on similar reactions³ has indicated that, at high temperatures, additional $O_2(b^1\Sigma_g^+)$ can be formed by direct excitation of $O_2(a^1\Delta_g)$



So reaction (10), the reverse of reaction (2), must be included in the analysis. Also with these quenchers,¹⁴ it is necessary to take into account the quenching of $O_2(a^1\Delta_g)$ which is deactivated appreciably during the observation time. The overall equation for the emission then becomes:

$$^{762}I = ^{762}I_{psg}(\rho_2/\rho_1) \int_{t-s_s}^t \{K \exp(-k_d[Q]t) + (1-K) \exp(-k_q[Q]t)\} \exp(-\beta t) dt/t_s. \quad (11)$$

The enhancement factor K consists of two terms:³

$$K = \frac{k_p}{(k_q - k_d)\chi} + \left(\frac{k'_q}{k_q}\right) \frac{1}{\chi} \left(\frac{[M]}{[\Delta]}\right)_{psg} \quad (12)$$

where χ , the ratio of the rate constants at room temperature, T_1 , is

$$\chi = \{k_p/(k_q - k_d + k_w^{\Sigma}/[M])\}_{T_1}. \quad (13)$$

The first term in eqn (12) is that used in the earlier work; the second results from the inclusion of reaction (10) in the analysis.³ The ratio (k'_q/k_q) is the equilibrium constant for reaction (2) which, taking the statistical weights of the two states into account, is:

$$(k'_q/k_q) = 0.5 \exp(-7555/T). \quad (13)$$

The ratio $[\Delta]/[M]$ is the fraction of $O_2(a^1\Delta_g)$ in the initial flow and is typically 4–5%.

Since the room-temperature rate constants as well as k_p and k_d are known, the experimental traces can be fitted to eqn (11) using non-linear least squares to yield values of k_q , t_s and β . β can be compared with the measured pre-shock decay; the integration time, t_s , was usually fixed in the analysis since it has been found before¹⁵ with efficient quenchers that t_s and k_q cannot both be well determined when the value of $k_q[Q]^{-1}$ is comparable with t_s . The measured rate constant is corrected to allow for quenching by oxygen itself to give k_q^Q , the rate constant for the quencher alone.

Fig. 5 and 6 show the results obtained for the quenching of $O_2(b^1\Sigma_g^+)$ by H_2 , D_2 and HCl . With H_2 and HCl the results from the different mixtures coalesce to give satisfactory lines which indicate the consistency of the analysis. Much difficulty was experienced with the D_2 mixtures; it is not so efficient a quencher and this appeared to give a large scatter in the results; only points for one mixture are shown. H_2 and D_2 are the first more-efficient quenchers to show an increase in k_q with temperature.

The results for HCl appear to decline slightly at high temperatures in a similar way to the behaviour found with other efficient quenchers;^{3,8,15} however, the general accuracy is such that one can only conclude that there is little change of k_q^{HCl} with temperature.

No results were obtained for mixtures with HBr at high temperatures, where the emission largely disappeared, showing only a noisy base-line in the post-shock region.

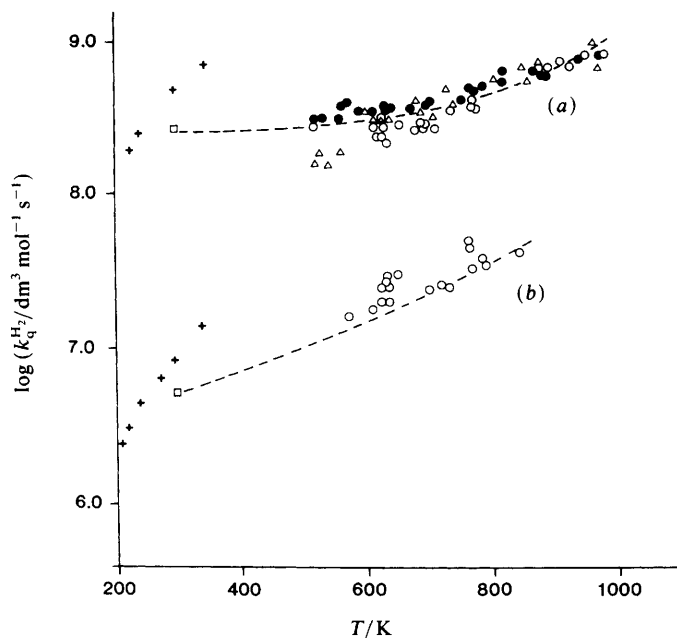


Figure 5. Plots of the rate constants for the quenching of $\text{O}_2(\text{b } ^1\Sigma_g^+)$ by H_2 (a) and D_2 (b) against temperature. Mixtures used: H_2 : \circ , 0.5%; \bullet , 1.0%; \triangle , 1% in a 3:1, O_2 - N_2 mixture; D_2 : \circ , 3%; \square , room temperature points; +, Kohse-Höinghaus and Stuhl.

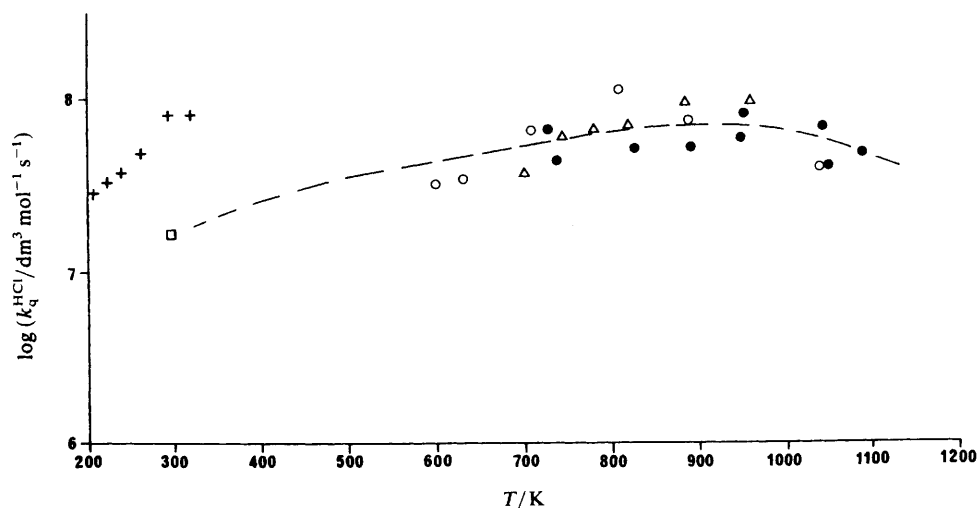


Fig. 6 Plot of the rate constants for the quenching of $\text{O}_2(\text{b } ^1\Sigma_g^+)$ by HCl . Mixtures used: \circ , 3%; \bullet , 5%; \triangle , 7%; \square , room-temperature points; +, Kohse-Höinghaus and Stuhl.

Above 1000 K, the 762 nm emission from mixtures with H₂, D₂ and also HCl showed an additional peak in the trace at long times as was observed at 634 nm.

Discussion

Empirical Features

The earlier measurements of the rate constant^{16–18} for the quenching of O₂(a ¹Δ_g) by H₂ at 295 K lie within the range $(2.5\text{--}3.2) \times 10^3 \text{ dm}^3 \text{ mol}^{-1} \text{ s}^{-1}$, which is much smaller than the present result, $(2.2 \pm 0.3) \times 10^4 \text{ dm}^3 \text{ mol}^{-1} \text{ s}^{-1}$. The previous results were obtained either by flash photolysis or by stopped flow in the Bonn sphere, and as oxygen was necessarily present they required the subtraction of a contribution due to the quenching by O₂, using the rate constant which has since been revised substantially downwards.^{16,19} Hence the earliest values are low, but even allowing for the later correction, our value is appreciably greater than can be accounted for by experimental uncertainty.

There are no other measurements of the quenching of O₂(a ¹Δ_g) by D₂, but it has already been indicated that the present result, $(2.6 \pm 1.3) \times 10^3 \text{ dm}^3 \text{ mol}^{-1} \text{ s}^{-1}$, is marred by the similarity in quenching efficiency between D₂ and O₂ itself and the low concentrations of D₂ used.

There have been 10 previous measurements of the rate constant for the quenching of O₂(b ¹Σ_g⁺) by H₂ at room temperature. As tabulated by Wayne,¹ the older measurements fall into two ranges: one lying in the range $(2.2\text{--}2.4) \times 10^8 \text{ dm}^3 \text{ mol}^{-1} \text{ s}^{-1}$ and the other in the range $(3.8\text{--}6.6) \times 10^8 \text{ dm}^3 \text{ mol}^{-1} \text{ s}^{-1}$. Our value of $(2.8 \pm 0.1) \times 10^8 \text{ dm}^3 \text{ mol}^{-1} \text{ s}^{-1}$ is in excellent agreement with the value of Singh and Setser²⁰ of $(2.7 \pm 1.0) \times 10^8 \text{ dm}^3 \text{ mol}^{-1} \text{ s}^{-1}$, but it is only half the most recent value of Michelangeli *et al.*²¹ obtained in a study of the quenching of O₂(b ¹Σ_g⁺) by hydrogen atoms.

For the quenching of O₂(b ¹Σ_g⁺) by D₂, the four previous determinations¹ of the rate constant lie in the range $(8.4\text{--}12.0) \times 10^6 \text{ dm}^3 \text{ mol}^{-1} \text{ s}^{-1}$. The present value, $(5.3 \pm 0.2) \times 10^6 \text{ dm}^3 \text{ mol}^{-1} \text{ s}^{-1}$, is appreciably lower, but in view of the quality of the results shown in fig. 3 and also the agreement of the present results for quenching by H₂, HCl and HBr with those of other workers, we prefer our value.

Our previously determined value for the rate constant for the quenching of O₂(b ¹Σ_g⁺) by HCl, $(1.6 \pm 0.2) \times 10^7 \text{ dm}^3 \text{ mol}^{-1} \text{ s}^{-1}$, also fell below the earlier values,¹ but is close to the value of Singh and Setser,²⁰ $(2.4 \pm 1.2) \times 10^7 \text{ dm}^3 \text{ mol}^{-1} \text{ s}^{-1}$.

Similarly, our new value, $(1.4 \pm 0.1) \times 10^8 \text{ dm}^3 \text{ mol}^{-1} \text{ s}^{-1}$, for the quenching of O₂(b ¹Σ_g⁺) by HBr, although being well above the early value of Braithwaite *et al.*,²² also agrees with that of Singh and Setser.²⁰

The results for the quenching of O₂(a ¹Δ_g) by H₂ and D₂ at high temperatures are shown as Arrhenius plots, as previous results have been for HCl, NO, SO₂ and O₂ itself.^{3,4,8,14} However, Plötz and Maier⁶ have shown that the low-temperature results for O₂ can be interpreted by a model which yields a curve on an Arrhenius plot while still fitting the results within experimental error. It is clear from fig. 3 and 4 that the scatter in the high-temperature results prevents any non-linearity from being discerned. Since the decay constant is determined from the subtraction of two similar values, the experimental error is magnified, and so it is difficult to reduce the scatter. This is the only technique suitable at the moment for obtaining results at high temperatures and gives reasonable estimates of the quenching constants, it cannot in this case yield values with sufficient accuracy to test the theoretical model.

As fig. 5 and 6 show, the rate constants for the quenching of O₂(b ¹Σ_g⁺) by H₂, D₂ and HCl are nearly independent of temperature between 295 and 1000 K and are thus similar³ to those of other more efficient quenchers of O₂(b ¹Σ_g⁺). Also shown are the results of Kohse-Höinghaus and Stuhl,²³ who studied the temperature dependence using flash photolysis with an H₂ laser to produce O(¹D) from O₂, which then reacts with O₂

to form $O_2(b\ ^1\Sigma_g^+)$. Their rate constants are rather high and show a steeper temperature dependence than would be expected from the extrapolation of the high-temperature results. It would be worth investigating the temperature dependence in more detail around room temperature to see whether the rate constant does in fact fall with temperature.

Theoretical Considerations

The contrast between the temperature dependences of the rate constants for quenching of the two states is marked for all of the quenchers studied: for $O_2(a\ ^1\Delta_g)$, the rate constants increase appreciably with temperature, having apparent activation energies of 10–30 kJ mol⁻¹, while the rate constants for $O_2(b\ ^1\Sigma_g^+)$ are nearly independent of temperature. It is surely this difference which any theoretical model must seek to explain.

The most successful approach to the problem is that of Plötz and Maier,⁶ who have studied the deactivation of both states by oxygen itself; in their model, the electronic energy is converted to vibrational energy in the two collision partners, and the most favoured channels are those in which the maximum amount of energy appears in vibration. They use the formulation of Shin²⁴ for vibrational relaxation to deal with the conversion of the excess energy to translation, and it is from this that the principal temperature dependence arises. By fitting the theory to one result at one temperature, they were able to fit some of the results and temperature dependences for both the a and b states in the two isotopic forms, $^{16}O_2$ and $^{18}O_2$.

Maier's approach is basically a 'resonance' transfer of energy between the electronic and vibrational degrees of freedom. Although it could encompass some of the results with polyatomic quenchers of $O_2(^1\Sigma_g^+)$, it is hard to see qualitatively how to explain the present results with H_2 and D_2 . The results for the other quenchers of $O_2(a\ ^1\Delta_g)$ also present a problem, since one would not expect the increases in rate constant with temperature which are observed.

Thomas and Thrush²⁵ analysed the results at a single temperature for a number of quenchers statistically, and obtained a common surprisal plot for both the a and b states. They concluded that, while much of the electronic energy does appear in vibration, resonant transfer is not important and that the mechanism is common and not specific to particular quenchers. Thus the question arises as to whether oxygen as a quencher is a special case and it is interesting to note that, as a quencher of $O_2(a\ ^1\Delta_g)$, it has a smaller temperature dependence^{4,6} than the other quenchers studied but that, as a quencher of $O_2(b\ ^1\Sigma_g^+)$, it has a larger one.^{7,8}

D.S.R. thanks the University of Keele for the award of a studentship and we thank Dr Patricia Borrell for her careful reading of the manuscript.

References

- 1 R. P. Wayne, in *Singlet Oxygen*, ed. A. A. Frimer (C.R.C. Press, Boca Raton, Fla., 1984), p.1.
- 2 R. B. Boodaghians, P. M. Borrell and P. Borrell, *J. Photochem.*, 1985, **31**, 29.
- 3 P. M. Borrell, P. Borrell, D. S. Richards and D. Quinney, *J. Chem. Soc., Faraday Trans. 2*, 1987, **83**, 2045.
- 4 A. P. Billington and P. Borrell, *J. Chem. Soc., Faraday Trans. 2*, 1986, **82**, 963.
- 5 M. Chatelet, A. Tardieu, W. Spreitzer and M. Maier, *Chem. Phys.*, 1986, **102**, 387.
- 6 J. Plötz and M. Maier, *Chem. Phys. Lett.*, 1987, **138**, 419.
- 7 P. M. Borrell, P. Borrell, M. D. Pedley and K. R. Grant, *Proc. R. Soc. London, Ser A*, 1979, **367**, 295.
- 8 P. Borrell, P. M. Borrell, D. S. Richards and R. B. Boodaghians, *J. Photochem.*, 1984, **25**, 399.
- 9 R. B. Boodaghians, P. M. Borrell and P. Borrell, *Chem. Phys. Lett.*, 1983, **97**, 193.
- 10 P. Borrell, *Comput. Chem.*, 1980, **4**, 131.
- 11 R. G. Derwent and B. A. Thrush, *Trans. Faraday Soc.*, 1971, **67**, 2036.
- 12 R. Boodaghians, P. Borrell, P. M. Borrell and D. S. Richards, *Bull. Soc. Chim. Belg.*, 1983, **92**, 1983.
- 13 J. P. Singh, J. Bachar, D. W. Setser and S. Rosenwaks, *J. Phys. Chem.*, 1985, **89**, 5347.

- 14 R. Boodaghians, P. M. Borrell and P. Borrell, *J. Chem. Soc., Faraday Trans. 2.*, 1983, **79**, 907.
- 15 P. M. Borrell, P. Borrell and K. R. Grant, *J. Chem. Phys.*, 1983, **78**, 748.
- 16 A. Leiss, U. Schurath, K. H. Becker and E. H. Fink, *J. Photochem.*, 1978, **8**, 211.
- 17 F. D. Findlay and D. R. Snelling, *J. Chem. Phys.*, 1971, **55**, 545.
- 18 R. J. Collins, R. J. Donovan and D. Husain, *J. Chem. Soc., Faraday Trans. 2*, 1973, **69**, 145.
- 19 P. Borrell, P. M. Borrell and M. D. Pedley, *Chem. Phys. Lett.*, 1977, **51**, 300.
- 20 J. P. Singh and D. W. Setser, *J. Phys. Chem.*, 1985, **89**, 5353.
- 21 D. V. Michelangeli, K. Y. Choo and M. T. Leu, *Int. J. Chem. Kinet.*, 1988, **20**, 915.
- 22 M. Braithwaite, E. A. Ogryzlo, J. A. Davidson and H. I. Schiff, *Chem. Phys. Lett.*, 1976, **42**, 158.
- 23 K. Kohse-Höinghaus and F. Stuhl, *J. Chem. Phys.*, 1980, **72**, 3720.
- 24 H. K. Shin, *J. Chem. Phys.*, 1965, **42**, 59.
- 25 R. G. O. Thomas and B. A. Thrush, *Proc. R. Soc. London, Ser. A*, 1977, **356**, 307.

Paper 8/04375B; Received 2nd November, 1988